

Reconstructing the Inflationary Landscape with Cosmological Data

Xingang Chen^a, Gonzalo A. Palma^b, Bruno Scheihing H.^b and Spyros Sypsas^b
^a*Institute for Theory and Computation, Harvard-Smithsonian Center for Astrophysics,
60 Garden Street, Cambridge, MA 02138, USA.*

^b*Grupo de Cosmología y Astrofísica Teórica, Departamento de Física,
FCFM, Universidad de Chile, Blanco Encalada 2008, Santiago, Chile.*

(Dated: October 17, 2018)

We show that the shape of the inflationary landscape potential may be constrained by analyzing cosmological data. The quantum fluctuations of fields orthogonal to the inflationary trajectory may have probed the structure of the local landscape potential, inducing non-Gaussianity (NG) in the primordial distribution of the curvature perturbations responsible for the cosmic microwave background (CMB) anisotropies and our Universe's large-scale structure. The resulting type of NG (tomographic NG) is determined by the shape of the landscape potential, and it cannot be fully characterized by 3- or 4-point correlation functions. Here we deduce an expression for the profile of this probability distribution function in terms of the landscape potential, and we show how this can be inverted in order to reconstruct the potential with the help of CMB observations. While current observations do not allow us to infer a significant level of tomographic NG, future surveys may improve the possibility of constraining this class of primordial signatures.

Is there any feature about our Universe that would require us to assume primordial non-Gaussian initial conditions? Up until now, cosmic microwave background (CMB) and large-scale structure (LSS) observations are fully consistent with the premise that the primordial curvature perturbations were initially distributed according to a perfectly Gaussian statistics [1, 2]. This has favored the simplest models of inflation—single field slow-roll inflation—based on the steady evolution of a scalar field driven by a flat potential [3–7]. In these models, the self-interactions of the primordial curvature perturbation lead to tiny non-Gaussianities suppressed by the slow-roll parameters characterizing the evolution of the Hubble expansion rate H , during inflation [8–11].

The confirmation of non-Gaussian initial conditions would help us to decipher certain fundamental aspects about inflation [12–15]. Indeed, non-Gaussianity (NG) can be generated by nonlinearities affecting the evolution of primordial curvature perturbations (denoted as ζ). These nonlinearities are the result of self-interactions, or interactions with other degrees of freedom, such as isocurvature fields (fields orthogonal to the inflationary trajectory in multifield space). Inevitably, perturbation theory limits the extent to which we can study the emergence of NG, forcing us to focus on the lowest order operators (in terms of field powers) in the ζ Lagrangian. Thus, most of the recent effort devoted to the study of NG has relied on parametrizing it with the bispectrum and trispectrum, the amplitudes of the 3- and 4-point correlation functions of ζ in momentum space. Understanding how different interactions lead to different shapes and runnings of the bispectrum has constituted one of the main programs in the study of inflation [12–15].

It is conceivable, however, that certain classes of interactions may lead to NG deviations that cannot be parametrized just with the bispectrum and/or trispectrum. This is the subject of the companion article [16],

where we argue that in multifield models characterized by a rich landscape structure (i.e., with minima separated by field distances of order, or smaller than, H), extra fields can transfer their NG to ζ . In two-field models, the mechanism by which this NG is generated relies on the existence of an isocurvature field ψ interacting with ζ via a generic coupling that appears in multifield models. The mechanism may be understood as the consequence of the following two independent statements:

- I. If on superhorizon scales the amplitude of ψ does not vanish, then it will act as a source for the amplitude of ζ . The field ζ will grow on superhorizon scales and become related to ψ (e.g., [17–19]).
- II. If ψ has a potential $\Delta V(\psi)$ with a rich structure, then around horizon crossing ψ will fluctuate and diffuse across the potential barriers. After horizon crossing, it will be more probable to measure ψ at values that minimize $\Delta V(\psi)$ [20].

Together, these two statements imply that the probability of measuring ζ is higher at those values sourced by ψ that minimize ΔV . This was shown in [16] for the particular case in which ψ is an axionlike field, with $\Delta V = \Lambda^4 [1 - \cos(\psi/f)]$. There, the main result consisted in the derivation of a probability distribution function (PDF) $\rho(\zeta)$ that depended explicitly on the barrier height Λ^4 and the field range f .

The purpose of this Letter is to extend the derivation of [16] to an arbitrary analytic potential ΔV , and to show how it is possible to reconstruct its shape with current and/or future cosmological data. Our main claim is that, if the primordial landscape had a rich structure, then its shape (around the inflationary trajectory) could be stored in the statistics of ζ through a type of NG (tomographic NG) that cannot be fully parametrized with the bispectrum alone.

Our starting point is to consider the following generic Lagrangian describing ζ and ψ ($M_{\text{Pl}} = 1$):

$$\mathcal{L} = a^3 \left[\epsilon (\dot{\zeta} - \alpha \dot{\psi})^2 - \frac{\epsilon}{a^2} (\nabla \zeta)^2 + \frac{1}{2} \dot{\psi}^2 - \frac{1}{2a^2} (\nabla \psi)^2 - \Delta V \right], \quad (1)$$

where a is the scale factor, and $\epsilon = -\dot{H}/H^2$ is the usual first slow-roll parameter ($H = \dot{a}/a$). In this system, ζ interacts with ψ via $\mathcal{L}_{\text{int}} \propto \alpha \zeta \dot{\psi}$ (with α constant). Note that we are treating both ζ and ψ up to quadratic order, except for ψ appearing in ΔV . We assume that $\Delta V/V_{\text{infl}} \ll 1$ so that inflation, driven by $V_{\text{infl}} = 3M_{\text{Pl}}^2 H^2$, is unaffected by ΔV . In what follows, \mathbf{x} and \mathbf{k} denote comoving position and momentum, whereas $\mathbf{q} = \mathbf{k}/a$ denotes physical momentum.

If $\Delta V = 0$, Eq. (1) gives us two linear equations of motion for ζ and ψ coupled through α . In k space, the dynamics is such that the mode function $\psi_k(t)$ becomes frozen to a constant value at horizon crossing. Then, ψ_k acts as a source for the amplitude of ζ_k , and one finds [19]

$$\zeta_k = (\alpha \Delta N / H) \psi_k, \quad (2)$$

where ΔN is the number of e -folds after horizon crossing. As a result, the power spectrum of ζ is determined by that of ψ as $P_\zeta(k) = \frac{\alpha^2 \Delta N^2}{H^2} P_\psi(k)$. Thus, the field ψ transfers its Gaussian statistics to ζ via α .

On the other hand, if $\Delta V \neq 0$, the field ψ continues to transfer its statistics to ζ (thanks to α), but this time it will inherit NG deviations. In momentum space, ΔV induces nonvanishing n -point correlation functions of the local type, given by

$$\langle \zeta_{\mathbf{k}_1 \dots \mathbf{k}_n}^n \rangle_c = (2\pi)^3 h_n \delta^{(3)} \left(\sum_{i=1}^n \mathbf{k}_i \right) \frac{k_1^3 + \dots + k_n^3}{k_1^3 \dots k_n^3}, \quad (3)$$

where c informs us that we are only keeping fully connected contributions (in the language of perturbation theory). To obtain the set of amplitudes h_n for an arbitrary potential we first consider the following Taylor expansion

$$\Delta V(\psi) = \sum_m \frac{c_m}{m!} \psi^m. \quad (4)$$

This expansion gives us an infinite number of m legged vertices, each one of order c_m . Using the in-in formalism, the computation of $\langle \zeta_{\mathbf{k}_1 \dots \mathbf{k}_n}^n \rangle_c$ requires us to consider the sum of each Feynman diagram proportional to c_{n+2m} with $m \geq 0$. In any such diagram, n legs become ζ external legs (due to the α coupling), whereas $2m$ legs become m loops. Finally, $\langle \zeta_{\mathbf{k}_1 \dots \mathbf{k}_n}^n \rangle_c$ is the result of summing all of these diagrams after taking into account the appropriate combinatorial factors. One finds

$$h_n = - \left(\frac{\alpha H \Delta N}{2} \right)^n \frac{\Delta N}{3H^4} \sum_{m=0}^{\infty} \frac{c_{n+2m}}{m!} \left(\frac{\sigma_0^2}{2} \right)^m, \quad (5)$$

where $\sigma_0^2 \equiv (2\pi)^{-3} \int d^3k \psi_k^*(t) \psi_k(t)$, appearing because of the loops, is the variance of the field ψ . Here, $\psi_k(t)$ is the mode function of a free massless field in a de Sitter spacetime. It turns out that σ_0^2 is time independent [20].

Performing the sum in Eq. (5), one obtains

$$\sum_{m=0}^{\infty} \frac{c_{n+2m}}{m!} \left(\frac{\sigma_0^2}{2} \right)^m = e^{\frac{\sigma_0^2}{2} \frac{\partial^2}{\partial \psi^2}} \Delta V \Big|_{\psi=0}. \quad (6)$$

Notice that σ_0^2 is formally infinite, and hence, we are forced to introduce infrared (IR) and ultraviolet (UV) physical momentum cutoffs. The UV cutoff q_{UV} corresponds to a wavelength well inside the horizon ($q_{\text{UV}} \gg H$), whereas the IR cutoff q_{IR} corresponds to the wavelength of the largest observable mode. In addition to these scales, it is convenient to introduce an arbitrary intermediate momentum q_L that splits σ_0^2 into two contributions: $\sigma_0^2 = \sigma_S^2 + \sigma_L^2$, from short and long modes, respectively. This splitting allows us to define a renormalized potential $\Delta V_{\text{ren}}(\psi) \equiv \exp\left(\frac{\sigma_S^2}{2} \frac{\partial^2}{\partial \psi^2}\right) \Delta V(\psi)$. In this way, observables can only depend on ΔV_{ren} , which is independent of q_{UV} .

According to Eq. (6), this renormalization procedure simply corresponds to defining $\Delta V_{\text{ren}}(\psi) = \sum_m c_m^{\text{ren}} \psi^m / m!$, where the coefficients c_m^{ren} are related to the bare couplings c_m as

$$\sum_{m=0}^{\infty} \frac{c_{n+2m}}{m!} \left(\frac{\sigma_0^2}{2} \right)^m = \sum_{m=0}^{\infty} \frac{c_{n+2m}^{\text{ren}}}{m!} \left(\frac{\sigma_L^2}{2} \right)^m. \quad (7)$$

This result allows us to identify ΔV_{ren} as the potential obtained by integrating out the high energy momenta beyond the scale q_L , just as in the Wilsonian approach of QFT. Now, it is crucial to notice that the n -point function of Eq. (3) is an observable, and so it cannot depend on q_L . This implies that h_n is independent of σ_L . For this to be possible, the coefficients c_m^{ren} defining ΔV_{ren} must run in such a way so that the entire expression (5) remains independent of σ_L . Equation (7) reveals how the coefficients c_m^{ren} run as more (or fewer) modes participate in σ_L^2 (again, in agreement with the Wilsonian picture).

To continue, using the Weierstrass transformation, the right hand side of Eq. (6) can be rewritten as

$$e^{\frac{\sigma_L^2}{2} \frac{\partial^2}{\partial \psi^2}} \Delta V_{\text{ren}} \Big|_{\psi=0} = \int d\psi \frac{e^{-\frac{\psi^2}{2\sigma_L^2}}}{\sqrt{2\pi\sigma_L}} \frac{\partial^n}{\partial \psi^n} \Delta V_{\text{ren}}. \quad (8)$$

Then, by performing several partial integrations, we finally obtain the following expression for h_n :

$$h_n = \frac{1}{n} \left(\frac{\alpha H \Delta N}{2\sigma_L} \right)^n \frac{\Delta N}{3H^4} \int d\psi \frac{e^{-\frac{\psi^2}{2\sigma_L^2}}}{\sqrt{2\pi\sigma_L}} \text{He}_n(\psi/\sigma_L) \times \left(\sigma_L^2 \frac{\partial^2}{\partial \psi^2} - \psi \frac{\partial}{\partial \psi} \right) \Delta V_{\text{ren}}(\psi), \quad (9)$$

where $\text{He}_n(x) \equiv \exp(-\frac{1}{2}x^2)x^n$ is the n th “probabilist’s” Hermite polynomial. In the particular case where $\Delta V(\psi) = \Lambda^4 [1 - \cos(\psi/f)]$, Eq. (9) allows us to recover the expression for $\langle \zeta_{\mathbf{k}_1 \dots \mathbf{k}_n}^n \rangle_c$ obtained in [16].

We now compute the n th moment $\langle \zeta^n \rangle$ for a particular position \mathbf{x} . Because of momentum conservation, the specific value of \mathbf{x} is irrelevant. In practice, we only have observational access to a finite range of scales, implying that the computation of $\langle \zeta^n \rangle$ must consider a window function selecting that range. We use a window function with a hard cutoff, and write

$$\zeta_L = \frac{1}{(2\pi)^3} \int_{k < k_L} d^3k \zeta_{\mathbf{k}} e^{-i\mathbf{k}\cdot\mathbf{x}}. \quad (10)$$

Notice that we have chosen to cut the integral with the same cutoff $k_L = a q_L$ introduced to split $\sigma_0^2 = \sigma_S^2 + \sigma_L^2$. Up until now, q_L was an arbitrary scale introduced to select the scales integrated out to obtain ΔV_{ren} . However, we can now choose q_L to coincide with the physical cutoff momentum setting the range of modes contributing to the computation of $\langle \zeta_L^n \rangle$. Given that we are interested in a q_L^{-1} larger than the horizon, we can write

$$\sigma_L^2 = (H^2/4\pi^2) \ln \xi, \quad (11)$$

where $\xi \equiv k_L/k_{\text{IR}}$. Following our companion paper [16], the n th moment of ζ_L is given by

$$\langle \zeta_L^n \rangle_c = (2\pi)^3 h_n I_n(\xi), \quad (12)$$

$$I_n(\xi) = \frac{n}{(2\pi^2)^{n+1}} \int_0^\infty \frac{dx}{x} G_\xi(x) [F_\xi(x)]^{n-1}, \quad (13)$$

where $G_\xi(x) = \int_{\xi^{-1}}^1 dz z x^2 \sin(zx)$ and $F_\xi(x) = \int_{\xi^{-1}}^1 \frac{dy \sin(yx)}{yx}$. The function $F_\xi(x)$ satisfies $F_\xi(0) = \ln \xi$, and $F_\xi(x) \leq \ln \xi$. The PDF $\rho(\zeta)$ must be such that

$$\langle \zeta_L^n \rangle = \int d\zeta \rho(\zeta) \zeta^n, \quad (14)$$

where $\langle \zeta_L^n \rangle$ is the full n th moment, including disconnected contributions, related to $\langle \zeta_L^n \rangle_c$ by $\langle \zeta_L^n \rangle = \sum_{m=0}^{\lfloor n/2 \rfloor} \frac{n!}{m!(n-2m)!2^m} \sigma_\zeta^{2m} \langle \zeta_L^{n-2m} \rangle_c$. Here, σ_ζ^2 is the variance of ζ , which according to Eqs. (2) and (11), is given by $\sigma_\zeta^2 = \alpha^2 \Delta N^2 \sigma_L^2 / H^2 = [\alpha^2 \Delta N^2 / (4\pi^2)] \ln \xi$. Planck fixes $\sigma_\zeta^2 / \ln \xi = P_\zeta(k) k^3 / (2\pi^2) = (2.196 \pm 0.158) \times 10^{-9}$.

To derive $\rho(\zeta)$ we just need to focus on the n dependence of $\langle \zeta^n \rangle_c$. According to Eq. (12), this dependence has the form $[X]^{n-1} \text{He}_n(Y)$, where X and Y are given quantities (the presence of the integrals do not alter this argument). This alone allows us to infer the PDF for ζ ,

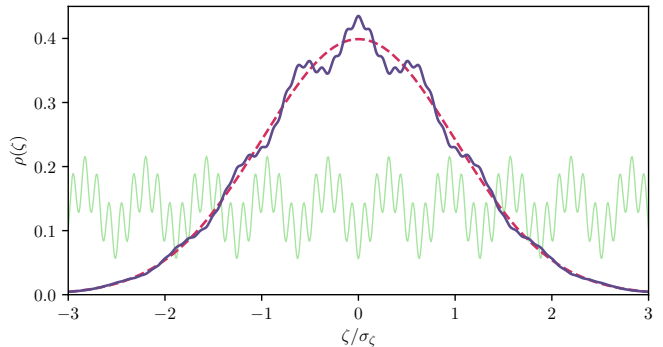


FIG. 1. The PDF (violet) resulting from a potential $\Delta V(\psi) \propto [2 - \cos(\psi/f_1) - \cos(\psi/f_2)]$, with $f_1 = 0.1\sigma_L$ and $f_2 = 0.02\sigma_L$ (light green). Both contributions have the same amplitude; however, f_2 contributes less than f_1 . A Gaussian PDF is plotted for comparison (red, dashed).

which is found to be given by

$$\rho(\zeta) = \frac{1}{\sqrt{2\pi}\sigma_\zeta} e^{-\frac{\zeta^2}{2\sigma_\zeta^2}} [1 + \Delta(\zeta)], \quad (15)$$

$$\Delta(\zeta) \equiv \int_0^\infty \frac{dx}{x} \mathcal{K}(x) \int_{-\infty}^\infty d\bar{\zeta} \frac{\exp\left[-\frac{(\bar{\zeta}-\zeta(x))^2}{2\sigma_\zeta^2(x)}\right]}{\sqrt{2\pi}\sigma_\zeta(x)} \times \frac{\Delta N}{3H^4} \left(\sigma_\zeta^2 \frac{\partial^2}{\partial \bar{\zeta}^2} - \bar{\zeta} \frac{\partial}{\partial \bar{\zeta}} \right) \Delta V_{\text{ren}}(\psi_{\bar{\zeta}}). \quad (16)$$

In the previous expression, $\Delta(\zeta)$ parametrizes the NG deviation. To write it, we defined the following quantities: $\zeta(x) \equiv [F_\xi(x)/\ln \xi]\zeta$, $\sigma_\zeta^2(x) \equiv \sigma_\zeta^2(1 - [F_\xi(x)/\ln \xi]^2)$, $\mathcal{K}(x) \equiv 4\pi G_\xi(x)/F_\xi(x)$, and $\psi_\zeta \equiv (\alpha \Delta N/H)^{-1}\zeta$. These definitions satisfy $|\zeta(x)| \leq |\zeta|$ and $\sigma_\zeta^2(x) \leq \sigma_\zeta^2$.

Equation (15) gives us the PDF of ζ at the end of inflation. It is possible to verify that the perturbativity condition on the potential is $\Delta V_{\text{ren}}/H^4 \ll 1$, and that the next to leading order term is of order $\mathcal{O}(\Delta^2)$ (see Ref. [16]). The presence of the derivative operator acting on ΔV_{ren} implies that the probability of measuring ζ at a given amplitude increases at those corresponding values ψ_ζ that minimize the potential. In addition, the x dependence of $\zeta(x)$ and $\sigma_\zeta^2(x)$ has the effect of filtering the structure; sharper structures contribute less to the PDF. Figure 1 shows the PDF obtained for a potential $\Delta V_{\text{ren}}(\psi) \propto [2 - \cos(\psi/f_1) - \cos(\psi/f_2)]$. In this example there are two sinusoidal contributions with field scales $f_1 = 0.1\sigma_L$ and $f_2 = 0.02\sigma_L$. Both contributions have the same amplitude, however, the NG deformation implied by f_2 is smaller than that of f_1 . Notice that to plot the figure, we used the relation $\psi_\zeta/\sigma_L = \zeta/\sigma_\zeta$.

Let us now attempt to reconstruct ΔV_{ren} out of the CMB data. This requires us to deal with the observed temperature fluctuation $\Theta \equiv \Delta T/T$, instead of ζ at the end of inflation. Thus, we introduce a linear transfer function to write $\Theta(\mathbf{k}, \hat{n}) \equiv T(k, \mu) \zeta_{\mathbf{k}}$, with $\mu = \hat{n} \cdot \hat{k}$,

where \hat{n} is the direction of sight of an observer standing at \mathbf{x} . It follows that $\langle \Theta_{\mathbf{k}_1 \dots \mathbf{k}_n}^n \rangle_c = T(k_1, \mu_1) \dots T(k_n, \mu_n) \langle \zeta_{\mathbf{k}_1 \dots \mathbf{k}_n}^n \rangle_c$, from which we are able to derive the connected n th moment:

$$\langle \Theta_L^n \rangle_c = (2\pi)^3 h_n (\sigma_\Theta / \sigma_\zeta)^n I_n^T(\xi), \quad (17)$$

where $I_n^T(\xi)$ is given by

$$I_n^T = \frac{n}{2(2\pi^2)^{n+1}} \int_{-1}^{+1} d\mu \int_0^\infty \frac{dx}{x} G_\xi^T(x, \mu) [F_\xi^T(x, \mu)]^{n-1}, \quad (18)$$

$$G_\xi^T = \frac{\sigma_\zeta}{\sigma_\Theta} \sum_\ell (2\ell + 1) P_\ell(\mu) \int_{\xi^{-1}}^1 dz z^2 x^3 T_\ell(zk_L) j_\ell(zx), \quad (19)$$

$$F_\xi^T = \frac{\sigma_\zeta}{\sigma_\Theta} \sum_\ell (2\ell + 1) P_\ell(\mu) \int_{\xi^{-1}}^1 \frac{dy}{y} T_\ell(yk_L) j_\ell(yx). \quad (20)$$

In the previous expressions, $P_\ell(x)$ and $j_\ell(x)$ stand for the ℓ th Legendre polynomial and ℓ th spherical Bessel function, respectively. In addition, T_ℓ is the Legendre moment of $T(k, \mu)$. The variance of Θ is found to be $\sigma_\Theta^2 = \frac{1}{4\pi} \sum_\ell (2\ell + 1) C_\ell$, with $C_\ell = 4\pi [\sigma_\zeta^2 / \ln \xi] \int_{k_{\text{IR}}}^{k_L} \frac{dk}{k} |T_\ell(k)|^2$.

One can now derive a PDF $\rho(\Theta)$ for Θ similar to that of Eqs. (15) and (16). However, we will not need an explicit expression for $\rho(\Theta)$ to engage in reconstructing ΔV . Instead, we may define the following cumulants parametrizing NG:

$$a_n \equiv \int d\Theta \rho(\Theta) \text{He}_n(\Theta / \sigma_\Theta). \quad (21)$$

Independently of the form of $\rho(\Theta)$, these coefficients are directly related to the fully connected moments of Θ through the relation $\langle \Theta_L^n \rangle_c = \sigma_\Theta^n a_n$. Together with (17), this further implies

$$h_n = a_n \sigma_\zeta^n / [(2\pi)^3 I_n^T(\xi)]. \quad (22)$$

Then, by expanding the potential in terms of Hermite polynomials $\Delta V_{\text{ren}}(\psi) / H^4 = \sum_m \frac{b_m}{m!} \text{He}_m(\psi / \sigma_L)$, one finds that the coefficients b_n determining the shape of the potential are given by

$$b_n = -\frac{3a_n}{(2\pi)^3 \Delta N I_n^T(\xi)} \left(\frac{\ln \xi}{2\pi^2} \right)^n. \quad (23)$$

The potential $\Delta V_{\text{ren}}(\psi)$ obtained by such a reconstruction has renormalized coefficients c_m^{ren} evaluated at the scale k_L , and so it can be interpreted as the potential generating NG in the range $k_{\text{IR}} \leq k \leq k_L$.

Having Eq. (23) at hand, we may proceed to outline the reconstruction process. Figure 2 shows values of the coefficients a_n acquired from Planck CMB maps (see also Ref. [21] for a similar analysis). The coefficients were obtained by counting the occurrences of Θ values in Planck's SMICA temperature map. Here we chose two possible values for σ_Θ^2 : the sample variance

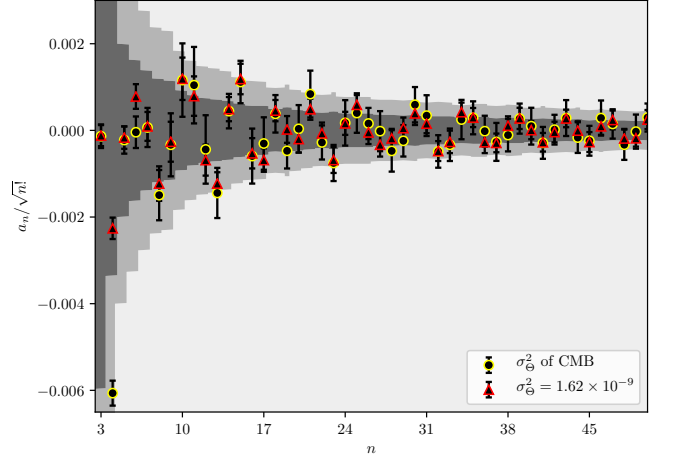


FIG. 2. The a_n coefficients obtained from Planck. We have limited the data to regions far enough from the galactic plane so that the outcome from SMICA agrees with the other pipelines (and removing each pipeline's masked pixels), effectively considering a third of the sky. The error bars are an estimate of the noise present in the data, computed by comparing half-mission maps. The grey contours represent the intrinsic noise $\sigma(a_n)$ due to Gaussian simulations obtained using full-sky maps generated with CAMB.

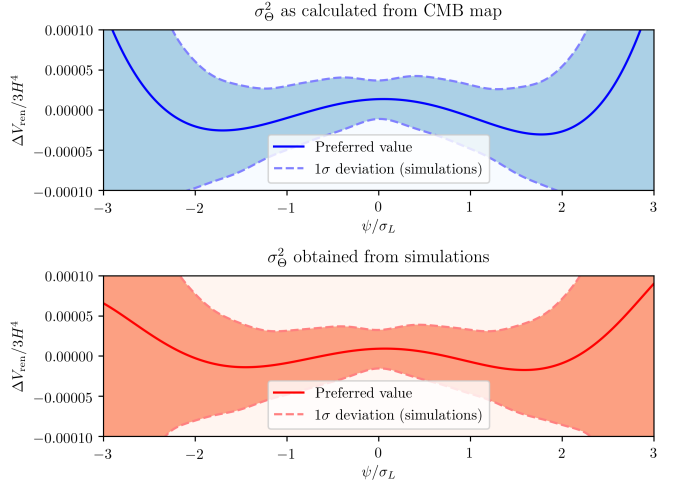


FIG. 3. The reconstructed potential $\Delta V / 3H^4$ for two different values of σ_Θ^2 . This reconstruction considers a_n coefficients up to $n = 7$. Since a_2 is a correction to the 2-point function – and hence, to the propagator – we do not include this term in the reconstructed potential.

computed from the CMB map $\sigma_\Theta^2 = 1.50 \times 10^{-9}$, with which $a_2 = 0$, and the one preferred by simulations $\sigma_\Theta^2 = 1.62 \times 10^{-9}$. The grey contours show the intrinsic noise $\sigma(a_n)$ (1- and 2- σ regions) resulting from 500 Gaussian simulations using CAMB [22] with the cosmological parameters reported by Planck [23] (with a beam resolution of 5 arcmin FWHM), and $\sigma_\Theta^2 = 1.62 \times 10^{-9}$, which is the average over simulations of the sample vari-

ances. As one might have expected, the observed values are mostly compatible with a Gaussian distribution. To get the b_n coefficients via Eq. (23), we set $\Delta N = 60$ and fix $\ln \xi = 8$, which corresponds to the range of momenta $10^{-4} \text{ Mpc}^{-1} \leq k \leq 0.3 \text{ Mpc}^{-1}$ for the observed modes in the CMB [24, 25]. Given that Fig. 2 lacks a conclusive imprint of non-Gaussianity, the potential in Fig. 3 serves for illustrative purposes only. However, we must note that this type of analysis is cosmic variance limited, as evidenced by the different results obtained from the two values chosen for $\sigma_{\mathcal{O}}^2$. Additionally, there are a number of anomalies present in the CMB that we disregard herein, such as the statistical differences between the north and south hemispheres [25]. Nevertheless, we encourage the community to keep an eye out for these signatures, as well as to perform more sophisticated analyses with available data sets. For instance, one approach to try and circumvent the aforementioned effects is to compute the transfer functions for a restricted multipole range, which can be done by modifying accordingly the sums in Eqs. (19) and (20), then to consider a filtered CMB map that only contains those contributions, and finally use Eq. (23) as before to obtain the reconstructed potential.

The NG studied here has a fixed shape of the local type [recall Eq. (3)], meaning that any relevant information is entirely contained in the coefficients h_n , related to the a_n 's via (22). However, the zero-lag cumulants approach offered in this Letter might not constitute the most efficient strategy to constrain the h_n 's. Shapes other than local, present in the data, will contribute to the measured a_n cumulants, increasing the uncertainty on the deduced values of the h_n 's. Hence, to break the shape degeneracy hidden in the cumulants, more sophisticated techniques may be considered. For instance, following similar steps to those described here, one could derive the full probability functional containing information about the local shape (or other shapes, in the case of nontrivial interactions not considered here) to perform reconstructions.

Our methods may be repeated to attempt reconstructions employing LSS, 21 cm, and CMB spectral distortion data. The main difference would rest on the treatment of specific transfer functions needed to connect the h_n 's with new a_n cumulants parametrizing new types of distributions (e.g., matter distribution in the case of LSS surveys). Granted that foregrounds and secondary NG's can be accurately modeled, these surveys should offer us the opportunity to perform better reconstructions of the landscape potential for the same reasons that they will improve upon current CMB constraints on the $f_{\text{NL}}^{\text{local}}$ parameter [i.e., reducing the uncertainty $\sigma(f_{\text{NL}}^{\text{local}})$]: they will give us access to a broader range of scales and/or larger data sets, allowing us to perform statistics with sharper cumulant uncertainties $\sigma(a_n)$. In this respect, it is worth recalling that soon to come LSS surveys will be able to reduce $\sigma(f_{\text{NL}}^{\text{local}})$ by a factor of 5 – 10 [26–28], whereas future 21 cm and CMB spectral distortion ex-

periments promise to do so by factors $\sim 10^2$ [29–31] and $\sim 10^3$ [32], respectively. An important pending challenge is to understand to what degree a reduction of $\sigma(f_{\text{NL}}^{\text{local}})$ will come together with a reduction of the $\sigma(a_n)$'s.

To summarize, we have analyzed a novel class of primordial signatures that deserves to be thoroughly studied both theoretically and observationally, particularly on the wake of new CMB [33] and LSS [34, 35] surveys. Multifield models of inflation allow for regimes in which the statistics of isocurvature fields are transferred to ζ , encoding information about the shape of the inflationary landscape potential in the observable curvature perturbations. We have considered a sufficiently generic situation described by the Lagrangian (1), however, the transfer mechanism might be even more generic, and as such, constraining this type of NG has an enormous potential for characterization of the early Universe.

Acknowledgments: We wish to thank Bastián Pradernas, Walter Riquelme and Domenico Sapone for useful discussions and comments. GAP and BSH acknowledge support from the Fondecyt Regular Project No. 1171811 (CONICYT). BSH is supported by a CONICYT Grant No. CONICYT-PFCHA/Magister Nacional/2018-22181513. SS is supported by the Fondecyt Postdoctorado Project No. 3160299 (CONICYT).

-
- [1] P. A. R. Ade *et al.* [Planck Collaboration], “Planck 2015 results. XVII. Constraints on primordial non-Gaussianity,” *Astron. Astrophys.* **594**, A17 (2016) [arXiv:1502.01592 [astro-ph.CO]].
 - [2] E. Komatsu *et al.* [WMAP Collaboration], “First year Wilkinson Microwave Anisotropy Probe (WMAP) observations: tests of gaussianity,” *Astrophys. J. Suppl.* **148**, 119 (2003) [astro-ph/0302223].
 - [3] A. H. Guth, “The Inflationary Universe: A Possible Solution to the Horizon and Flatness Problems,” *Phys. Rev. D* **23**, 347 (1981).
 - [4] A. A. Starobinsky, “A New Type of Isotropic Cosmological Models Without Singularity,” *Phys. Lett. B* **91**, 99 (1980).
 - [5] A. D. Linde, “A New Inflationary Universe Scenario: A Possible Solution of the Horizon, Flatness, Homogeneity, Isotropy and Primordial Monopole Problems,” *Phys. Lett. B* **108**, 389 (1982).
 - [6] A. Albrecht and P. J. Steinhardt, “Cosmology for Grand Unified Theories with Radiatively Induced Symmetry Breaking,” *Phys. Rev. Lett.* **48**, 1220 (1982).
 - [7] V. F. Mukhanov and G. V. Chibisov, “Quantum Fluctuations and a Nonsingular Universe,” *JETP Lett.* **33**, 532 (1981) [*Pisma Zh. Eksp. Teor. Fiz.* **33**, 549 (1981)].
 - [8] A. Gangui, F. Lucchin, S. Matarrese and S. Mollerach, “The Three point correlation function of the cosmic microwave background in inflationary models,” *Astrophys. J.* **430**, 447 (1994) [astro-ph/9312033].
 - [9] E. Komatsu and D. N. Spergel, “Acoustic signatures in the primary microwave background bispectrum,” *Phys. Rev. D* **63**, 063002 (2001) [astro-ph/0005036].

- [10] V. Acquaviva, N. Bartolo, S. Matarrese and A. Riotto, “Second order cosmological perturbations from inflation,” *Nucl. Phys. B* **667**, 119 (2003) [astro-ph/0209156].
- [11] J. M. Maldacena, “Non-Gaussian features of primordial fluctuations in single field inflationary models,” *JHEP* **0305**, 013 (2003) [astro-ph/0210603].
- [12] N. Bartolo, E. Komatsu, S. Matarrese and A. Riotto, “Non-Gaussianity from inflation: Theory and observations,” *Phys. Rept.* **402**, 103 (2004) [astro-ph/0406398].
- [13] M. Liguori, E. Sefusatti, J. R. Fergusson and E. P. S. Shellard, “Primordial non-Gaussianity and Bispectrum Measurements in the Cosmic Microwave Background and Large-Scale Structure,” *Adv. Astron.* **2010**, 980523 (2010) [arXiv:1001.4707 [astro-ph.CO]].
- [14] X. Chen, “Primordial Non-Gaussianities from Inflation Models,” *Adv. Astron.* **2010**, 638979 (2010) [arXiv:1002.1416 [astro-ph.CO]].
- [15] Y. Wang, “Inflation, Cosmic Perturbations and Non-Gaussianities,” *Commun. Theor. Phys.* **62**, 109 (2014) [arXiv:1303.1523 [hep-th]].
- [16] X. Chen, G. A. Palma, W. Riquelme, B. Scheiring Hitschfeld and S. Sypsas, “Landscape tomography through primordial non-Gaussianity,” arXiv:1804.07315 [hep-th].
- [17] C. Gordon, D. Wands, B. A. Bassett and R. Maartens, “Adiabatic and entropy perturbations from inflation,” *Phys. Rev. D* **63**, 023506 (2001) [astro-ph/0009131].
- [18] X. Chen and Y. Wang, “Quasi-Single Field Inflation and Non-Gaussianities,” *JCAP* **1004**, 027 (2010) [arXiv:0911.3380 [hep-th]].
- [19] A. Achúcarro, V. Atal, C. Germani and G. A. Palma, “Cumulative effects in inflation with ultra-light entropy modes,” *JCAP* **1702**, no. 02, 013 (2017) [arXiv:1607.08609 [astro-ph.CO]].
- [20] G. A. Palma and W. Riquelme, “Axion excursions of the landscape during inflation,” *Phys. Rev. D* **96**, no. 2, 023530 (2017) [arXiv:1701.07918 [hep-th]].
- [21] T. Buchert, M. J. France and F. Steiner, “Model-independent analyses of non-Gaussianity in Planck CMB maps using Minkowski functionals,” *Class. Quant. Grav.* **34**, no. 9, 094002 (2017) [arXiv:1701.03347 [astro-ph.CO]].
- [22] <https://camb.info>
- [23] P. A. R. Ade *et al.* [Planck Collaboration], “Planck 2015 results. XIII. Cosmological parameters,” *Astron. Astrophys.* **594**, A13 (2016) [arXiv:1502.01589 [astro-ph.CO]].
- [24] P. A. R. Ade *et al.* [Planck Collaboration], “Planck 2015 results. XX. Constraints on inflation,” *Astron. Astrophys.* **594**, A20 (2016) [arXiv:1502.02114 [astro-ph.CO]].
- [25] P. A. R. Ade *et al.* [Planck Collaboration], “Planck 2015 results. XVI. Isotropy and statistics of the CMB,” *Astron. Astrophys.* **594**, A16 (2016) [arXiv:1506.07135 [astro-ph.CO]].
- [26] C. Carbone, O. Mena and L. Verde, “Cosmological Parameters Degeneracies and Non-Gaussian Halo Bias,” *JCAP* **1007**, 020 (2010) [arXiv:1003.0456 [astro-ph.CO]].
- [27] O. Doré *et al.*, “Cosmology with the SPHEREX All-Sky Spectral Survey,” arXiv:1412.4872 [astro-ph.CO].
- [28] A. Raccanelli, M. Shiraishi, N. Bartolo, D. Bertacca, M. Liguori, S. Matarrese, R. P. Norris and D. Parkinson, “Future Constraints on Angle-Dependent Non-Gaussianity from Large Radio Surveys,” *Phys. Dark Univ.* **15**, 35 (2017) [arXiv:1507.05903 [astro-ph.CO]].
- [29] A. Loeb and M. Zaldarriaga, “Measuring the small - scale power spectrum of cosmic density fluctuations through 21 cm tomography prior to the epoch of structure formation,” *Phys. Rev. Lett.* **92**, 211301 (2004) [astro-ph/0312134].
- [30] J. B. Muñoz, Y. Ali-Hamoud and M. Kamionkowski, “Primordial non-gaussianity from the bispectrum of 21-cm fluctuations in the dark ages,” *Phys. Rev. D* **92**, no. 8, 083508 (2015) [arXiv:1506.04152 [astro-ph.CO]].
- [31] P. D. Meerburg, M. Münchmeyer, J. B. Muñoz and X. Chen, “Prospects for Cosmological Collider Physics,” *JCAP* **1703**, no. 03, 050 (2017) [arXiv:1610.06559 [astro-ph.CO]].
- [32] E. Pajer and M. Zaldarriaga, “A New Window on Primordial non-Gaussianity,” *Phys. Rev. Lett.* **109**, 021302 (2012) [arXiv:1201.5375 [astro-ph.CO]].
- [33] K. N. Abazajian *et al.* [CMB-S4 Collaboration], “CMB-S4 Science Book, First Edition,” arXiv:1610.02743 [astro-ph.CO].
- [34] <http://sci.esa.int/euclid/>
- [35] <https://www.lsst.org/>